

University of Texas Rio Grande Valley

ScholarWorks @ UTRGV

---

Earth, Environmental, and Marine Sciences  
Faculty Publications and Presentations

College of Sciences

---

11-2019

## Increasing impacts of extreme droughts on vegetation productivity under climate change

Chonggang Xu

Nate G. McDowell


Rosie A. Fisher

Liang Wei

Sanna Sevanto

*See next page for additional authors*

Follow this and additional works at: [https://scholarworks.utrgv.edu/eems\\_fac](https://scholarworks.utrgv.edu/eems_fac)

 Part of the [Earth Sciences Commons](#), [Environmental Sciences Commons](#), and the [Marine Biology Commons](#)

---

### Recommended Citation

Xu, Chonggang, Nate G. McDowell, Rosie A. Fisher, Liang Wei, Sanna Sevanto, Bradley O. Christoffersen, Ensheng Weng, and Richard S. Middleton. 2019. "Increasing Impacts of Extreme Droughts on Vegetation Productivity under Climate Change." *Nature Climate Change* 9 (12): 948–53. <https://doi.org/10.1038/s41558-019-0630-6>.

This Article is brought to you for free and open access by the College of Sciences at ScholarWorks @ UTRGV. It has been accepted for inclusion in Earth, Environmental, and Marine Sciences Faculty Publications and Presentations by an authorized administrator of ScholarWorks @ UTRGV. For more information, please contact [justin.white@utrgv.edu](mailto:justin.white@utrgv.edu), [william.flores01@utrgv.edu](mailto:william.flores01@utrgv.edu).

---

**Authors**

Chonggang Xu, Nate G. McDowell, Rosie A. Fisher, Liang Wei, Sanna Sevanto, Bradley O. Christoffersen, Engsheng Weng, and Richard S. Middleton

1                   **INCREASING IMPACTS OF EXTREME DROUGHTS ON VEGETATION**  
2                   **PRODUCTIVITY UNDER CLIMATE CHANGE**

3                   Chonggang Xu<sup>1\*</sup>, Nate G. McDowell<sup>2</sup>, Rosie A. Fisher<sup>3,4</sup>, Liang Wei<sup>1,5</sup>, Sanna Sevanto<sup>1</sup>,  
4                   Bradley O. Christoffersen<sup>6</sup>, Ensheng Weng<sup>7</sup>, Richard Middleton<sup>1</sup>

5  
6                   **Affiliations:**

7  
8                   1: Earth and Environmental Sciences Division, Los Alamos National Laboratory, Los Alamos,  
9                   NM, USA;

10                  2: Earth Systems Analysis & Modeling Division, Pacific Northwest National Laboratory,  
11                  Richland, WA, USA;

12                  3: Climate and Global Dynamics, National Center for Atmospheric Research, Boulder, CO,  
13                  USA;

14                  4: Centre Européen de Recherche et de Formation Avancée en Calcul Scientifique (CERFACS),  
15                  Toulouse, France;

16                  5: Key Laboratory of Western China's Environmental Systems, College of Earth and  
17                  Environmental Sciences, Lanzhou University, Lanzhou, Gansu, China;

18                  6: Department of Biology and School of Earth, Environmental, and Marine Sciences, The  
19                  University of Texas Rio Grande Valley, Edinburg, TX, USA;

20                  7: Center for Climate Systems Research, Columbia University, and NASA Goddard Institute for  
21                  Space Studies, New York, NY, USA

22                  \*Correspondence to: [cxu@lanl.gov](mailto:cxu@lanl.gov)

23

24 **Abstract:** Terrestrial gross primary production (GPP) is the basis of food production and  
25 vegetation growth globally<sup>1</sup>, and plays a critical role in regulating atmospheric CO<sub>2</sub> through its  
26 impact on ecosystem carbon balance. Even though higher CO<sub>2</sub> concentrations in future decades  
27 can increase GPP<sup>2</sup>, low soil water availability, heat stress, and disturbances associated with  
28 droughts could reduce the benefits of such CO<sub>2</sub> fertilization. Here we analyzed outputs of 13  
29 Earth System Models (ESMs) to show an increasingly stronger impact on GPP by extreme  
30 droughts than mild and moderate droughts over the 21<sup>st</sup> century. Due to a dramatic increase in  
31 the frequency of extreme droughts, the magnitude of globally-averaged reductions in GPP  
32 associated with extreme droughts was projected to be nearly tripled by the last quarter of this  
33 century (2075–2099) relative to that of the historical period (1850–1999) under both high and  
34 intermediate greenhouse gas emission scenarios. In contrast, the magnitude of GPP reduction  
35 associated with mild and moderate droughts was not projected to increase substantially. Our  
36 analysis indicates a high risk of extreme droughts to the global carbon cycle with atmospheric  
37 warming; however, this risk can be potentially mitigated by positive anomalies of GPP  
38 associated with favorable environmental conditions.

39

40           The terrestrial biosphere absorbed ~30% of anthropogenic carbon emissions from fossil  
41 fuels during 1990–2007<sup>3</sup>, making it a critical component of the global carbon sink that mitigates  
42 fossil fuel CO<sub>2</sub> emissions and associated climate warming. GPP is a measure of fixation of CO<sub>2</sub>  
43 into an ecosystem through photosynthesis and plays a key role in the net carbon balance of the  
44 terrestrial biosphere and the terrestrial CO<sub>2</sub> absorption. However, despite our knowledge of CO<sub>2</sub>  
45 fertilization effects on plant productivity<sup>2</sup>, the future trend of GPP under elevated CO<sub>2</sub> levels  
46 remains highly uncertain due to the impact of many factors such as nutrient limitation<sup>4</sup> and  
47 increasing frequency and intensity of drought<sup>5</sup>. Drought is already the most widespread factor  
48 affecting GPP<sup>6</sup> via direct physiological impacts such as water limitation and heat stress<sup>7</sup>, and  
49 through its indirect impacts on increased frequency and intensity of disturbances such as fire and  
50 insect outbreaks<sup>8</sup> that release large amounts of carbon back into the atmosphere. In agreement  
51 with such trends, several modeling studies have showed an increasing risk of a greater frequency  
52 and intensity of droughts in many regions during the 21<sup>st</sup> century<sup>9-12</sup>, which could affect the  
53 magnitude of future GPP and lead to high uncertainty in projecting the future of terrestrial  
54 carbon sink. Previous studies have assessed the importance of different climate factors for carbon  
55 flux extremes<sup>13,14</sup>, but few studies have specifically quantified future drought impacts on GPP at  
56 the global scale.

57           To better understand how future drought will affect GPP at the global scale, we analyzed  
58 the climate and GPP projections from 13 ESMs in the Coupled Model Intercomparison Project  
59 Phase 5 (CMIP5)<sup>15</sup>. The models were selected based on the criteria that they reported both soil  
60 water content at different depths and GPP, to quantify the potential impacts of droughts on future  
61 terrestrial GPP. Given that plant responses to water stress depend on their historical climate  
62 conditions<sup>16</sup>, we defined location (i.e., grid cell for ESMs) and model-specific droughts during

63 the historical period of 1850–1999 as months when plant accessible soil water (PASW: vertical  
64 integral of soil water weighted by the fraction of roots in a soil column at different depths) was  
65 less than the 10<sup>th</sup> percentile for each location. These percentile-defined droughts may not have an  
66 impact on GPP at very wet sites, therefore, we only used the 10<sup>th</sup> percentile to define droughts if  
67 GPP during these drought months was significantly lower (with a significance level of 0.01) than  
68 that of the non-drought months (see Methods and Extended data Fig. 1 for details). We classified  
69 droughts into extreme, moderate, and mild so that PASW was less than the 2<sup>nd</sup> percentile during  
70 extreme droughts, between the 5<sup>th</sup> and 2<sup>nd</sup> percentiles during moderate droughts, and between the  
71 10<sup>th</sup> and 5<sup>th</sup> percentiles during mild droughts. Projected future droughts were sorted into these  
72 categories using the grid-cell-, model-, and month-specific historical simulations. The drought-  
73 associated change in GPP was calculated based on the deviations (or anomalies) of GPP from the  
74 mean for each month of a specific location during 1850-2099 (See Methods and Extended data  
75 Fig. 1 for details). Positive deviations from the mean indicate that droughts stimulate GPP and  
76 negative deviations indicate that droughts reduce GPP.

77 Our analysis showed that drought events defined by low PASW were projected to  
78 become more frequent under future climates (Fig. 1). The frequency of extreme droughts per  
79 year was projected to increase by a factor of ~3.8 (p-value < 0.001) under the high greenhouse  
80 gas emission scenario (RCP 8.5<sup>15</sup>) and by a factor of ~3.1 (p-value < 0.001) under the  
81 intermediate greenhouse gas emission scenario (RCP 4.5<sup>15</sup>) (Fig. 1a, b) during 2075–2099,  
82 compared to the historical period of 1850–1999. The mean frequency of moderate droughts per  
83 year was projected to increase by a factor of ~1.2 (not significant with p-value > 0.2) under  
84 scenario RCP8.5 (Fig. 1d) and by a factor of ~1.5 (p-value < 0.01) under scenario RCP4.5 (Fig.  
85 1c). One reason for the relatively lower increase of moderate drought frequency under scenario

86 RCP8.5 in comparison to scenario RCP 4.5 was that drought events became more extreme under  
87 scenario RCP8.5 and thus there was a smaller proportion of moderate drought events under this  
88 scenario (Extended data Fig. 2). These droughts were widely distributed with particularly high  
89 risks for the Amazon, South Africa, Mediterranean Basin, Australia, and southwest USA (Fig.  
90 2). The risk of mild droughts did not change significantly in the future (Fig. 1e, f). The drought  
91 events were typically associated with low humidity (Extended data Fig. 3), low precipitation  
92 (Extended data Fig. 4), high temperature (Extended data Fig. 5), high radiation (Extended data  
93 Fig. 6), and increased carbon release from fire disturbances (Extended data Fig. 7).

94 The magnitude of annual GPP reductions associated with droughts was also projected to  
95 increase substantially in the future (Fig. 3). In terms of absolute carbon fluxes, the magnitude of  
96 forecasted mean reductions in global GPP associated with droughts will rise from ~2.8 Pg C per  
97 year during 1850–1999 to ~4.5 and ~4.7 Pg C per year (p-value <0.01) during 2075–2099 under  
98 emission scenario RCP8.5 and RCP 4.5, respectively (Extended data Fig. 8). Drought-associated  
99 reductions in GPP (Figs. 3 and 4) can arise in two main ways: 1) via an increased intensity of  
100 droughts (in terms of GPP impact), or 2) via an increased drought frequency. Our analysis  
101 showed that the ensemble mean of absolute GPP reduction per drought event was not projected  
102 to be significantly larger in the future (Extended data Fig. 9). This could result from the effect of  
103 CO<sub>2</sub> fertilization for the both drought and non-drought months (see next paragraph for details).  
104 Therefore, the increasing impact of drought upon GPP mainly resulted from the increased  
105 frequency of drought events. Due to the relatively large increase in the frequency of extreme  
106 droughts (Fig. 1), the magnitude of GPP reductions associated with extreme droughts increased  
107 much more than that associated with moderate and mild droughts in the future (Fig. 3).  
108 Specifically, the magnitude of annual GPP reduction associated with extreme droughts during

109 2075–2099 was projected to increase by a factor of  $\sim 2.9$  ( $p$ -value  $< 0.001$ ) and  $\sim 2.7$  ( $p$ -value  $<$   
110  $0.001$ ) under emission scenarios of RCP8.5 and RCP4.5, respectively (Fig. 3 a, b), compared to  
111 their historical mean values during 1850–1999. In contrast, no significant increase in the  
112 magnitude of mean GPP reduction was detected for mild and moderate droughts except for the  
113 moderate droughts under RCP4.5 (Fig. 3 c-e). Therefore, the proportion of total GPP reduction  
114 contributed by extreme droughts was projected to increase from  $\sim 28\%$  during 1850–1999 to  $\sim 56$   
115 and  $49\%$  during 2075–2099 under emission scenarios RCP 8.5 and RCP4.5, respectively  
116 (Extended data Fig. 10). The projected GPP reductions associated with droughts were correlated  
117 with changes in several environmental drivers including PASW, temperature, humidity and  
118 radiation, and vegetation states with each variable contributing  $\sim 10$ – $30\%$  on average  
119 (Supplementary Fig. 1 and Supplementary Fig. 2).

120 The GPP reduction associated with droughts can be viewed in the context of rising GPP  
121 under future CO<sub>2</sub> fertilization, which was included in all selected Earth system model  
122 projections. Due to CO<sub>2</sub> fertilization and higher temperature for high latitudes, the globally-  
123 averaged mean GPP was projected to be  $\sim 50\%$  and  $\sim 31\%$  higher for year 2075–2099 compared  
124 to the historical period (1850–1999) under emission scenarios of RCP 8.5 and RCP 4.5,  
125 respectively (Supplementary Fig. 3). Similarly, the GPP in drought periods was also projected to  
126 increase significantly for mild and moderate droughts ( $p$ -value  $< 0.02$ ) but not significantly for  
127 extreme droughts (Supplementary Fig. 4). To better understand the drought impacts in relative  
128 terms, we calculated the impacts of droughts as the percentages reduction in GPP associated with  
129 droughts. The percentage reduction averaged across all models showed no significant change  
130 during 2075–2099 compared to the historical period during 1850–1999 under RCP 8.5  
131 (Supplementary Fig. 5 a). Under the emission scenario of RCP 4.5, percentage reduction of GPP



132 by droughts was projected to have a slight increase from ~1.8% per year during 1850–1999 to  
133 ~2.3% per year (p-value < 0.01) in 2075–2099 (Supplementary Fig. 5b). Relative to RCP 4.5, the  
134 lower percentage reduction in GPP during 2075–2099 under RCP 8.5 could result from the  
135 beneficial impact of higher CO<sub>2</sub> concentrations on plant production during moderate and mild  
136 droughts (e.g., higher photosynthetic rate and increased water use efficiency with lower stomata  
137 conductance<sup>2</sup>) (Supplementary Fig. 6 c-e). For both mild and moderate droughts, the magnitude  
138 of percentage reduction in GPP decreased except for moderate drought under RCP4.5  
139 (Supplementary Fig. 6 c-e). However, for extreme droughts, the percentage reduction in GPP  
140 was projected to be doubled (p-value < 0.001) under both emission scenario RCP 8.5 and RCP  
141 4.5 (Supplementary Fig. 6 a, b). This suggests that the magnitude of extreme-drought-associated  
142 GPP reduction increases faster than the mean GPP in the future.

143         There was a large latitudinal variation in the projected impact of drought on GPP. The  
144 drought impacts on GPP for years 2075–2099 (measured by the grid-cell-specific GPP reduction  
145 relative to the historical period of 1850–1999) were much larger in tropical and temperate  
146 regions and smaller at high latitudes (Fig. 4; see Supplementary Fig. 7 for a reference over years  
147 1975–1999). The uncertainty was also relatively lower for tropical and temperate regions as  
148 measured by the relative amount of deviation from the ensemble mean (Supplementary Fig. 8  
149 and Supplementary Fig. 9). The large increase in the magnitude of drought-associated reduction  
150 in GPP projected for tropical and temperate regions (Fig. 4) is in agreement with recent  
151 observations of drought-associated vegetation changes in Europe<sup>17</sup>, the Amazon basin<sup>18</sup>, Western  
152 US<sup>19,20</sup>, and the global assessment of drought-induced plant production reduction during 1999–  
153 2009 using remote-sensing-based estimates<sup>21</sup>. The small impacts of droughts on GPP at high  
154 latitudes could result from their relatively low GPP and beneficial consequences of higher

155 temperature (Extended data Fig. 5) and radiation (Extended data Fig. 6) during the drier months  
156 in these colder regions<sup>22</sup>, where relatively high antecedent soil moisture buffers vegetation  
157 against stress-inducing drought levels despite experiencing statistically dry conditions. However,  
158 this projection of small GPP reductions at high latitudes could be too optimistic given that all the  
159 current ESMs do not explicitly consider insect dynamics, which are influenced by drought and  
160 warming climate and have substantial impacts on regional to global carbon cycles<sup>23,24</sup>. Long-  
161 term observational data also showed that drought had already led to substantial tree mortality  
162 across Canada from 1963–2008<sup>25</sup>.

163         The ESMs projected not only an increase of mean GPP in the future due to CO<sub>2</sub>  
164 fertilization (Supplementary Fig. 3), but also an increase of variability in GPP (Supplementary  
165 Fig. 10). This suggests that magnitude of both positive and negative anomalies around the mean  
166 of GPP will increase in the future<sup>14</sup>. The GPP reduction associated with drought represents one  
167 of the key drivers of negative abnormalities for the simulated GPP in ESMs; however, at global  
168 scale, these negative anomalies could be mitigated by the positive anomalies of GPP related to  
169 wet conditions, favorable temperature and radiation, and enhanced water use efficiency due to  
170 elevated CO<sub>2</sub> concentration<sup>2</sup>. Zscheischler et al<sup>14</sup> pointed out that the dominance of large  
171 negative carbon extremes (e.g., deviation of GPP from the mean) could be changed toward  
172 dominance of large positive carbon extremes in GPP in the 21<sup>st</sup> century. Thus, it is possible that  
173 the high risk of increasing impact of extreme droughts on GPP could be mitigated by the positive  
174 impacts on GPP in the future under favorable environmental conditions of temperature, soil  
175 moisture and radiation.

176 **References**

- 177 1 Imhoff, M. L. *et al.* Global patterns in human consumption of net primary production. *Nature*  
178 **429**, 870-873, doi:10.1038/nature02619 (2004).
- 179 2 Long, S. P., Ainsworth, E. A., Rogers, A. & Ort, D. R. Rising atmospheric carbon dioxide: plants  
180 face the future. *Annu Rev Plant Biol* **55**, 591-628 (2004).
- 181 3 Le Quere, C. *et al.* Global Carbon Budget 2018. *Earth Syst Sci Data* **10**, 2141-2194,  
182 doi:10.5194/essd-10-2141-2018 (2018).
- 183 4 Norby, R. J., Warren, J. M., Iversen, C. M., Medlyn, B. E. & McMurtrie, R. E. CO<sub>2</sub> enhancement of  
184 forest productivity constrained by limited nitrogen availability. *Proc Natl Acad Sci U S A* **107**,  
185 19368-19373, doi:10.1073/pnas.1006463107 (2010).
- 186 5 Allen, C. D., Breshears, D. D. & McDowell, N. G. On underestimation of global vulnerability to  
187 tree mortality and forest die-off from hotter drought in the Anthropocene. *Ecosphere* **6**, Art n  
188 129, doi:10.1890/Es15-00203.1 (2015).
- 189 6 Reichstein, M. *et al.* Climate extremes and the carbon cycle. *Nature* **500**, 287-295,  
190 doi:10.1038/Nature12350 (2013).
- 191 7 Pinheiro, C. & Chaves, M. Photosynthesis and drought: can we make metabolic connections  
192 from available data? *J Exp Bot* **62**, 869-882, doi:10.1093/jxb/erq340 (2010).
- 193 8 Williams, A. P. *et al.* Temperature as a potent driver of regional forest drought stress and tree  
194 mortality. *Nature Clim. Change* **3**, 292-297, doi:10.1038/nclimate1693 (2013).
- 195 9 Sillmann, J., Kharin, V. V., Zwiers, F. W., Zhang, X. & Bronaugh, D. Climate extremes indices in the  
196 CMIP5 multimodel ensemble: Part 2. Future climate projections. *J Geophys Res-Atmos* **118**,  
197 2473-2493, doi:Doi 10.1002/Jgrd.50188 (2013).
- 198 10 Burke, E. J., Brown, S. J. & Christidis, N. Modeling the recent evolution of global drought and  
199 projections for the twenty-first century with the hadley centre climate model. *J Hydrometeorol*  
200 **7**, 1113-1125, doi:Doi 10.1175/Jhm544.1 (2006).
- 201 11 Cook, B. I., Ault, T. R. & Smerdon, J. E. Unprecedented 21st century drought risk in the American  
202 Southwest and Central Plains. *Science Advances* **1**, e1400082, doi:10.1126/sciadv.1400082  
203 (2015).
- 204 12 Boisier, J. P., Ciais, P., Ducharne, A. & Guimberteau, M. Projected strengthening of Amazonian  
205 dry season by constrained climate model simulations. *Nat Clim Change* **5**, 656-660,  
206 doi:10.1038/Nclimate2658 (2015).
- 207 13 Frank, D. *et al.* Effects of climate extremes on the terrestrial carbon cycle: concepts, processes  
208 and potential future impacts. *Glob Change Biol* **21**, 2861-2880, doi:10.1111/gcb.12916 (2015).
- 209 14 Zscheischler, J. *et al.* Carbon cycle extremes during the 21st century in CMIP5 models: Future  
210 evolution and attribution to climatic drivers. *Geophys Res Lett* **41**, 2014GL062409,  
211 doi:10.1002/2014GL062409 (2015).
- 212 15 Taylor, K. E., Stouffer, R. J. & Meehl, G. A. An Overview of CMIP5 and the Experiment Design. *B*  
213 *Am Meteorol Soc* **93**, 485-498, doi:10.1175/Bams-D-11-00094.1 (2012).
- 214 16 Choat, B. *et al.* Global convergence in the vulnerability of forests to drought. *Nature* **491**, 752-+,  
215 doi:Doi 10.1038/Nature11688 (2012).
- 216 17 Ciais, P. *et al.* Europe-wide reduction in primary productivity caused by the heat and drought in  
217 2003. *Nature* **437**, 529-533, doi:10.1038/nature03972 (2005).
- 218 18 Doughty, C. E. *et al.* Drought impact on forest carbon dynamics and fluxes in Amazonia. *Nature*  
219 **519**, 78-U140, doi:10.1038/nature14213 (2015).
- 220 19 Breshears, D. D. *et al.* Regional vegetation die-off in response to global-change-type drought.  
221 *Proc Natl Acad Sci U S A* **102**, 15144-15148, doi:10.1073/pnas.0505734102 (2005).

222 20 van Mantgem, P. J. & Stephenson, N. L. Apparent climatically induced increase of tree mortality  
223 rates in a temperate forest. *Ecol Lett* **10**, 909-916, doi:10.1111/j.1461-0248.2007.01080.x  
224 (2007).

225 21 Zhao, M. & Running, S. W. Drought-induced reduction in global terrestrial net primary  
226 production from 2000 through 2009. *Science* **329**, 940-943, doi:10.1126/science.1192666  
227 (2010).

228 22 Kattge, J. & Knorr, W. Temperature acclimation in a biochemical model of photosynthesis: a  
229 reanalysis of data from 36 species. *Plant Cell Environ* **30**, 1176-1190, doi:10.1111/j.1365-  
230 3040.2007.01690.x (2007).

231 23 Hicke, J. A. *et al.* Effects of biotic disturbances on forest carbon cycling in the United States and  
232 Canada. *Glob Change Biol* **18**, 7-34, doi:10.1111/j.1365-2486.2011.02543.x (2012).

233 24 Hicke, J. A., Meddens, A. J. H., Allen, C. D. & Kolden, C. A. Carbon stocks of trees killed by bark  
234 beetles and wildfire in the western United States. *Environ Res Lett* **8**, doi:10.1088/1748-  
235 9326/8/3/035032 (2013).

236 25 Peng, C. *et al.* A drought-induced pervasive increase in tree mortality across Canada's boreal  
237 forests. *Nature Clim. Change* **1**, 467-471, doi:10.1038/nclimate1293 (2011).

238

239 *Methods*

240 We selected 13 ESM simulations (Supplementary Table 1) from CMIP5 archive, based  
241 on the criteria that they reported both soil water at different soil depths and GPP. There are  
242 multiple simulations for each ESM under each specific greenhouse gas emission scenarios. In  
243 this study, we selected only the first reported simulation for each model, given that multiple  
244 inclusions of the same model might lead to its over-representation in our analysis<sup>26</sup>. We also  
245 collected additional climate variables including precipitation, radiation, temperature and relative  
246 humidity to identify the deviations in climate for drought months from the same CMIP5 archive.  
247 In this study, we only considered two emission scenarios: RCP8.5 and RCP4.5. This was  
248 justified by the fact that these scenarios generally capture the potential range of future  
249 greenhouse gas releases and that fewer simulations are available for other emission scenarios.

250 There are many ways to define droughts<sup>11</sup>. Because our goal was to understand impacts  
251 of drought on GPP, we used plant accessible soil water (PASW) as an indicator of drought.  
252 PASW was defined as the sum of soil water weighted by the fractions of plant roots at different  
253 soil depths (see Supplementary Note 1 for details). Because drought tolerance of plants depends  
254 on their historical climate conditions<sup>16</sup>, we defined droughts based on the site-specific PASW.  
255 Specifically, we defined a month in a specific year as a month of mild, moderate, and extreme  
256 drought if its PASW was less than (or equal to) the 10<sup>th</sup> but larger than the 5<sup>th</sup> percentile, less  
257 than (or equal to) the 5<sup>th</sup> but large than the 2<sup>nd</sup> percentile, and less than (or equal to) the 2<sup>nd</sup>  
258 percentile for the same month during 1850–1999, respectively (Extended data Fig. 1a). These  
259 percentiles were then used to identify months of different levels of droughts during 2000–2099  
260 based on the projected PASW. Even if PASW of a certain month was relatively low (e.g., <10<sup>th</sup>  
261 percentile) for a specific year, it may not have an impact on plant production if the site was very

262 wet. Thus, we used these percentiles to define droughts only if GPP values of a specific month  
263 for the years with PASW less than the 10th percentile were significantly lower than the rest of  
264 years during 1850–2099 (see Supplementary Note 1, Supplementary Fig. 11, and Supplementary  
265 Fig. 12 for details).

266 In most models, each grid cell can contain more than one plant functional type (PFT)  
267 with differing root distributions. Ideally, we could have defined droughts based on whether the  
268 PASW of a PFT had a significant impact on the PFT-specific GPP; however, the CMIP5  
269 database only has a single total GPP for each specific grid cell. In this study, droughts were thus  
270 defined by PASW of different PFTs as long as GPP during the defined drought months was  
271 significantly lower than that during non-drought months (see Supplementary Note 1 for details of  
272 statistical tests). This does not affect our analysis because all the droughts defined by PASW of  
273 different PFTs had a significant impact on the lumped GPP. If a specific month was set as  
274 drought month by PASW of multiple PFTs, however, we defined the drought category based on  
275 the PASW of the PFT that had the most significant impact on GPP (see Supplementary Note 1  
276 for details).

277 To quantify drought impacts on GPP, we first fitted a smooth spline over noisy  
278 simulations of GPP for a specific month (e.g., May) during 1850–2099 (Extended data Fig. 1b).  
279 See Supplementary Note 2 for details of smooth spline estimations. This spline was then used to  
280 represent the mean GPP for the month of interest. For each drought month, the deviation (or  
281 anomaly) of its GPP from the estimated spline was used to quantify the monthly impact of  
282 drought on GPP (Supplementary Note 3 and Extended data Fig. b). Finally, we summed these  
283 deviations across months and spatial locations to estimate impacts of the drought on GPP at the  
284 global scale. The corresponding standard errors were estimated based on the standard errors of

285 the estimated spline (see Supplementary Note 2 for details). Statistical tests were used to test for  
286 significant differences in drought risks and associated GPP reductions (see Supplementary Note  
287 5 for details). Our approach might underestimate drought impacts, because drought-associated  
288 GPP reduction could plausibly extend past the end of the duration of drought defined based on  
289 soil moisture<sup>13,27</sup>. Further studies based on specific model experiments are needed to identify  
290 these lag impacts, because it is difficult to confirm if the follow-on reductions in GPP result from  
291 the lag effects of droughts or other environmental condition changes (e.g., low radiation) in the  
292 CMIP5 archive.

293 It is important to point out that the PASW is only one indicator of drought. The impact of  
294 droughts on GPP can be attributed to different climate variables such as temperature, humidity,  
295 radiation, precipitation, and PASW, and to different vegetation states such as PFT compositions,  
296 height, and leaf area index. To understand the importance of different climate variables and  
297 vegetation states on GPP reductions associated with droughts, we fitted multilinear regressions to  
298 estimated GPP deviations with explanatory variables of PASW, daily temperature, incoming  
299 solar radiation, relative humidity, and mean GPP (as an indicator of overall vegetation status) for  
300 all the drought events for a specific month for the 25-year periods during 1850–2099 (see  
301 Supplementary Note 4 for details).

### 302 ***Data Availability***

303 The ESM output data that support the findings of this study are available from the CMIP5 site  
304 (<https://esgf-node.llnl.gov/projects/cmip5/>).

### 305 ***Code availability***

306 The processing R codes are available from corresponding author upon request.

307

308 ***METHODS REFERENCES***

- 309 26 Sanderson, B. M., Knutti, R. & Caldwell, P. A Representative Democracy to Reduce  
310 Interdependency in a Multimodel Ensemble. *J Climate* **28**, 5171-5194, doi:10.1175/Jcli-D-14-  
311 00362.1 (2015).
- 312 27 Anderegg, W. R. L. *et al.* Pervasive drought legacies in forest ecosystems and their implications  
313 for carbon cycle models. *Science* **349**, 528-532, doi:10.1126/science.aab1833 (2015).

314

315



316 **ENDNOTES**

317 Please contact Chonggang Xu (cxu) for correspondence and requests for materials.

318 **Acknowledgments**

319           This work was funded by the NGEE Tropics project and the Survival/ Mortality (SUMO)  
320 project sponsored by the DOE Office of Science, Office of Biological and Environmental  
321 Research, the Los Alamos National Laboratory LDRD program, and the UC-Lab Fees Research  
322 Program (grant no. LFR-18-542511). This submission is under public release with the approved  
323 LA-UR-14-23309. We thank Dave Lawrence and Charlie Koven for their helpful feedback on  
324 the initial manuscript and two anonymous reviewers for their helpful comments for the revision.  
325 We thank Nancy Kiang from NASA Goddard Institute for Space Studies for sharing the PFT  
326 distribution map in GISS models, Paul Milly from NOAA's Geophysical Fluid Dynamics  
327 Laboratory (GFDL) for sharing the PFT distribution in GFDL's Earth System Models, and Jerry  
328 Tjiputra from University of Bergen for sharing the PFT distributions in NorESM models for this  
329 study. We also acknowledge the World Climate Research Programme's Working Group on  
330 Coupled Modelling, which is responsible for CMIP, and we thank the climate modeling groups  
331 (Supplementary Table 1) for producing and making available their model output. For CMIP, the  
332 U.S. Department of Energy's Program for Climate Model Diagnosis and Intercomparison  
333 provides coordinating support and led development of software infrastructure in partnership with  
334 the Global Organization for Earth System Science Portals.

335

336 **Author Contributions**

337 All authors contributed to the manuscript writing. CX and NGM initially designed the  
338 experiment. CX implemented the analysis. LW helped data exploration for evaluating the  
339 results; RAF, SS, BOC and RM provide suggestions for improvement of the experimental design  
340 and analysis. EW provided support on water limitation functions and PFT mapping on GFDL  
341 and NOAA models.

342 **Competing Interests statement**

343 We declare that no competing interests are present in the manuscript.

344

345 **Figure legends**

346 **Fig. 1 Temporal changes in annual drought frequency relative to the historical period of**  
347 **1850–1999.** The relative frequencies were calculated on a model-specific basis, dividing the  
348 projected mean annual drought frequency (drought events/year) for a specific period (e.g., years  
349 2075–2099) by that over the historical period. Values  $<1$  indicate that the drought frequency  
350 decreases while values  $>1$  indicate that the drought frequency increases compared to the  
351 historical period. The P-values were calculated using the bootstrap sampling (see Supplementary  
352 Note 5.2 for details) to test if the mean frequency across different models during 2075–2099  
353 were significantly higher than the historical period. The gray horizontal line represents the  
354 ensemble mean for 2075–2099. See Supplementary Table 1 for the abbreviations of 13 selected  
355 Earth system models.

356 **Fig. 2 Spatial distribution of drought frequency during 2075–2099 relative to the historical**  
357 **period of 1850–1999.** The relative frequencies were averaged over the ensemble of 13 Earth  
358 system models. They were calculated on a model- and grid-cell-specific basis, dividing the mean  
359 drought frequency per year (drought events/year) during 2075–2099 by that over the historical  
360 period. Values  $<1$  indicate the drought frequency decreases while values  $>1$  indicate that the  
361 drought frequency increases compared to the historical period. The frequencies projected by  
362 different models were interpolated to a reference spatial resolution [ $1.125^\circ$  (longitude)  $\times$   $0.9375^\circ$   
363 (latitude)] for mapping purposes.

364 **Fig. 3 Temporal changes in GPP anomalies associated with droughts relative to the**  
365 **historical period of 1850–1999.** The relative anomalies were calculated on a model-specific  
366 basis, dividing the mean annual GPP anomaly associated with droughts ( $\text{kg C/m}^2/\text{year}$ ) for a  
367 specific period (e.g., years 2075–2099) by that for the historical period (see Methods and

368 Supplementary Note 3). They were multiplied by (-1) to indicate that droughts decrease GPP,  
369 with -1 indicating the reference drought-associated GPP anomaly for the historical period.  
370 Hence, values  $< -1$  indicate that the magnitude of GPP reduction becomes larger relative to the  
371 historical period, while values  $> -1$  indicate that the magnitude of GPP reduction becomes  
372 smaller. The dotted line shows the mean relative anomaly during 2075–2099 across all models.  
373 The P-values were calculated using the bootstrap sampling (see Supplementary Note 5.2 for  
374 details) to test if the mean magnitude of GPP reduction during 2075–2099 across different  
375 models becomes significantly larger than that during the historical period. See Supplementary  
376 Table 1 for the abbreviations of 13 selected Earth system models.

377 **Fig. 4 Spatial distribution of GPP anomalies associated with droughts during 2075–2099**  
378 **relative to the historical period of 1850–1999.** The relative anomalies were averaged over the  
379 ensemble of 13 Earth system models. They were calculated on a model basis, dividing the grid-  
380 cell-specific mean annual GPP anomalies ( $\text{kg C/m}^2/\text{year}$ ) during 2075–2099 by the global mean  
381 annual GPP reduction ( $\text{kg C/m}^2/\text{year}$ ) for the historical period. The relative anomalies were  
382 multiplied by (-1) to indicate that droughts decrease GPP, with -1 indicating the reference global  
383 mean GPP reduction for the historical period. Hence, values  $< -1$  (shades of red) indicate that the  
384 magnitude of GPP reduction was larger than the global mean GPP reduction during the historical  
385 period, while values  $> -1$  (light blue) indicate that the magnitude of GPP reduction was smaller.  
386 The drought-associated changes in GPP projected by different models were interpolated to a  
387 reference spatial resolution [ $1.125^\circ$  (longitude)  $\times$   $0.9375^\circ$  (latitude)] for mapping purposes.